

See discussions, stats, and author profiles for this publication at: <https://www.researchgate.net/publication/268926245>

Plasmon Resonance Hybridization of Gold Nanospheres and Palladium Nanoshells Combined in a Rattle Structure

ARTICLE in JOURNAL OF PHYSICAL CHEMISTRY LETTERS · JULY 2014

Impact Factor: 7.46 · DOI: 10.1021/jz501201p

CITATIONS

3

READS

21

1 AUTHOR:



Mahmoud A. Mahmoud

Georgia Institute of Technology

76 PUBLICATIONS 1,808 CITATIONS

[SEE PROFILE](#)

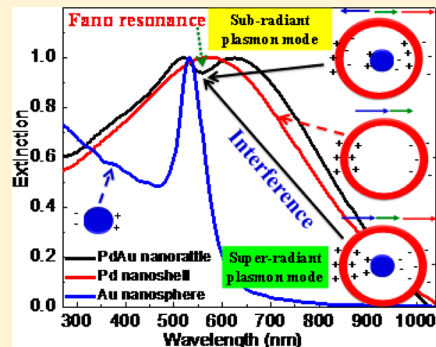
Plasmon Resonance Hybridization of Gold Nanospheres and Palladium Nanoshells Combined in a Rattle Structure

Mahmoud A. Mahmoud*

Laser Dynamics Laboratory, School of Chemistry and Biochemistry, Georgia Institute of Technology, 901 Atlantic Drive, Atlanta, Georgia 30332-0400, United States

Supporting Information

ABSTRACT: Gold and palladium nanoparticles are characterized by their localized surface plasmon resonance (LSPR). In contrast with the sharp LSPR spectrum of gold nanoparticles, palladium nanoparticles had a broad LSPR spectrum. Palladium–gold nanorattles (PdAuNRT) are an ideal system with optical properties that are a hybrid of gold and palladium nanoparticles. The PdAuNRTs consisted of small gold nanospheres (AuNSs) located inside hollow palladium nanospheres (PdHNSs) of larger sizes without touching each other. PdAuNRTs of various sizes were synthesized by systematic variation of the experimental parameters. Interestingly, for the PdAuNRTs, where PdHNSs and AuNSs are separated by a distance, it was found that the broad plasmon resonance band of the PdHNSs hybridizes with the sharp plasmon resonance of the AuNSs located in its center. This was further confirmed experimentally by optical absorption measurements and theoretically using discrete dipole approximation technique. The plasmon resonance hybridization resulted in broadening of the LSPR spectrum of the PdAuNRTs and the appearance of a dip due to a Fano resonance.



SECTION: Plasmonics, Optical Materials, and Hard Matter

Localized surface plasmon resonance (LSPR) is one of the exciting properties of the metallic nanoparticles, which has been widely used for many applications.^{1–4} Upon excitation of the conduction-band-free electrons of the metallic nanoparticles by electromagnetic radiation of resonance frequency, they oscillate and that generates plasmon field and LSPR extinction spectrum.⁵ The plasmon field can enhance different radiative and nonradiative processes, which are mainly based on electronic transitions. The LSPR spectrum acts as a lens that intensifies the photons in a nanometer area by the scattering part of the LSPR^{6,7} or generates photothermal heat by the absorption part of LSPR.⁸ The size, shape, and composition of plasmonic nanoparticles have been engineered appropriately for enhancing the target property of the electronic system by the nanoparticles.^{9–11} This engineering accounts for the LSPR peak position, the scattering to absorption spectrum ratio, and the plasmon field intensity.^{12–14}

The width of the LSPR spectrum of the plasmonic nanoparticles is inversely proportional to the coherence time (the time that the oscillated electrons stay in-phase before damping).¹⁵ The oscillated electron cloud generates dipolar charge,⁵ and damping of the dipolar charge oscillation is proportional to the square of the second derivative of the dipole moment.⁵ Any factor affects the damping of the dipolar charge oscillation of the plasmonically excited nanoparticles, such as the composition, shape, size, the dielectric function of the surrounding medium, and proximity of other nanoparticles will affect the width of the LSPR spectrum and the resonance

frequency as well.^{3,16} Gold and silver nanoparticles produce sharp LSPR spectrum, due to their long coherence time, while the LSPR spectrum of platinum and palladium nanoparticles, especially those of hollow structures, are broad and cover both the visible and UV regions.^{17–19} Combining gold nanoparticles with platinum and palladium nanoparticles have improved their optical properties as observed in the gold–palladium and gold platinum shell–shell nanoparticles.¹⁸ This interesting combination between these metallic nanoparticles did not show any improvement in the optical properties of the gold nanoparticles. But, the mechanical properties of the soft gold nanoparticles found to be enhanced.²⁰ Mixing of the plasmonic nanoparticles encourage the possibility of the plasmon resonance hybridization and a remarkable change in their optical properties.²¹ Fano resonance was observed as a dip in the LSPR spectrum when a dark plasmon mode of one of the plasmonic nanoparticles interferes with a broad bright mode of the other plasmonic nanoparticle.²² In fact, both the bright and dark mode most likely resulted from the hybridization of the plasmon modes of the nanoparticles. The plasmon resonance hybridization and Fano resonance were observed in concentric nanoparticles of either similar shapes and different sizes such as multilayer concentric nanoshells^{23,24} or nanoparticles of different shapes and sizes as in the concentric ring-disc

Received: June 11, 2014

Accepted: July 18, 2014

Published: July 18, 2014



nanocavities.²⁵ Plasmon hybridization and Fano-resonance were also discussed for separated nanoparticles of either similar shapes and sizes, such as in the case of plasmon field coupling of four nanorods²⁶ and in heptamer nanodiscs²² or different shapes and different sizes, for example, nanoshells and nanospheres heterodimers.²⁷ In all of these examples discussing the plasmon resonance hybridization, nanoparticles of similar composition were used. Recently, numerical simulation has been used successfully to predict the plasmon resonance hybridization in palladium–silver nanorod dimers of asymmetric lengths, and signatures of Fano interferences in the electron energy loss spectroscopy and cathodoluminescence were observed.²⁸ This letter discusses the plasmon resonance hybridization in the palladium–gold nanorattle (PdAuNRT), where small gold nanospheres (AuNSs) are introduced inside larger palladium hollow nanospheres (PdHNSs). Newly prepared PdAuNRT was synthesized with three different sizes based on the galvanic replacement technique. Experimental measurements and theoretical calculations using the discrete dipole approximation (DDA) technique showed one LSPR peak for both PdHNSs and AuNSs. However, the measured and simulated LSPR spectrum of PdHNSs is broad, but the AuNSs spectrum is sharp. The position of the AuNSs LSPR peak is located at the center of the broad spectrum of PdHNSs. Interestingly, PdAuNRTs showed a slightly broader LSPR spectrum compared with that of separated PdHNS, in addition to a dip in the spectrum, observed at a wavelength longer than the LSPR peak position of AuNSs. Plasmon hybridization model is used successfully to describe the reason for the broadening of the LSPR spectrum of the PdAuNRTs as well as the dip in the spectrum.

Palladium–gold nanorattles were prepared with different sizes by technique similar to the gold nanorattles previously reported.²⁹ In brief, gold nanospheres were prepared first by the citrate reduction of the gold salt,³⁰ followed by deposition of a silver shell around the gold nanosphere by citrate reduction of the silver ion.²⁹ The PdAuNRTs were obtained by replacing the silver atoms, forming the nanoshell coating the gold nanospheres, by palladium atoms through a galvanic replacement reaction between palladium ions and silver atoms. (The detailed procedure is given in the Supporting Information.) However, two silver atoms will be replaced by one palladium atom, which caused the formation of a palladium shell separated by vacancy from the AuNSs. Silver nanospheres have been used as a template in the galvanic replacement during the synthesis of PdHNSs (Supporting Information). Ocean Optics HR4000Cg-UV-NIR was used to conduct the optical measurements of the colloidal nanoparticles. A JEOL 100C transmission electron microscope (TEM) was used for TEM imaging, while Tecnai F30 was used for high-resolution TEM imaging. Figure 1A shows the TEM image of PdHNSs with a diameter of 55.5 ± 6.3 nm. The TEM images of PdAuNRTs of AuNSs with diameters of 16.5 ± 2.5 , 29.8 ± 2.4 , and 65.1 ± 11.7 nm and outer PdHNSs with diameters of 41.6 ± 5.2 , 77.5 ± 7.2 , and 148 ± 15 nm, are shown in Figure 1B–D, respectively. For careful characterization of the PdAuNRTs, HRTEM imaging was conducted. The HRTEM image of PdAuNRT in Figure 1E is for 40.8 nm diameter and 3.2 nm wall thickness; the inner AuNS is 17.1 nm in diameter. It is clear that the AuNS does not adhere with the inner wall of the palladium shell. Upon magnification of the right-top area of the HRTEM image in Figure 1 E to include a section from the gold nanosphere and part from the wall of palladium shell, the lattice

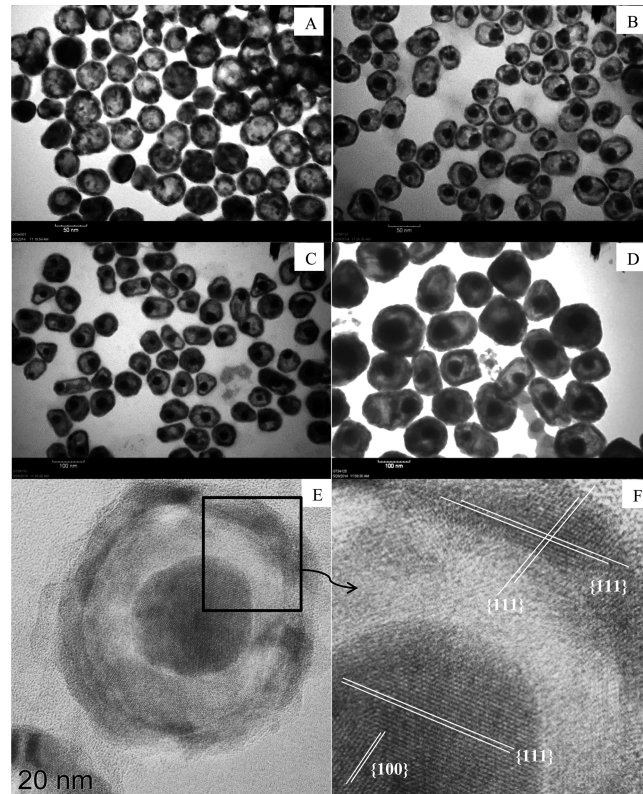


Figure 1. TEM images of (A) 55.5 ± 6.3 nm palladium hollow spheres, (B) palladium–gold nanorattles of 41.6 ± 5.2 nm outer palladium nanoshell and 16.5 ± 2.5 nm inside gold nanospheres, (C) 29.8 ± 2.4 nm inside gold nanospheres and 77.5 ± 7.2 nm outer palladium nanoshells, and (D) 65.1 ± 11.7 nm inside nanospheres and 148 ± 15 nm outer palladium nanoshells. (E) High-resolution TEM image of PdAuNRT of 40.8 nm diameter and 3.2 nm wall thickness; the inner AuNS is 17.1 nm in diameter. (F) Lattice-resolved image of PdAuNRTs.

d spacing can be determined. (See Figure 1F.) From the lattice-resolved image, the lattice *d* spacing was found to be 0.23 and 0.200 nm for gold AuNS, which correspond to the {111} and {100} facets, respectively, while the palladium wall showed a value of lattice *d* spacing of 0.22 nm assigned for the {111} facet.

The DDA technique (DDSCAT 6.1) was used to calculate the LSPR spectrum and the electromagnetic plasmon field of the AuNSs, PdHNSs, and PdAuNRTs. The shape files of the PdHNSs and PdAuNRTs in the DDA calculation contain three holes, and one dipole is generated per 1 nm^2 . The dielectric function of the surrounding medium was taken in the calculation to be the average of water and polyvinylpyrrolidone. The electromagnetic plasmon fields were calculated for the plane of $y = 0.6x$ length of the PdAuNRT.

Each plasmonic nanoparticle has its characteristic optical properties that change upon their proximity to other plasmonic nanoparticles.⁵ PdAuNRTs are complex plasmonic systems for the following reasons: (1) They are made of two different metals (Pd and Au), (2) their structure is different because AuNSs have solid structure with one plasmonic surface while PdHNSs are hollow with two plasmonic surfaces, and (3) the AuNSs sitting inside the shell could possibly adhere to the inner wall of the PdHNSs or move freely. To study the optical properties of the newly prepared PdAuNRTs, the optical properties of the AuNSs and PdHNSs are addressed

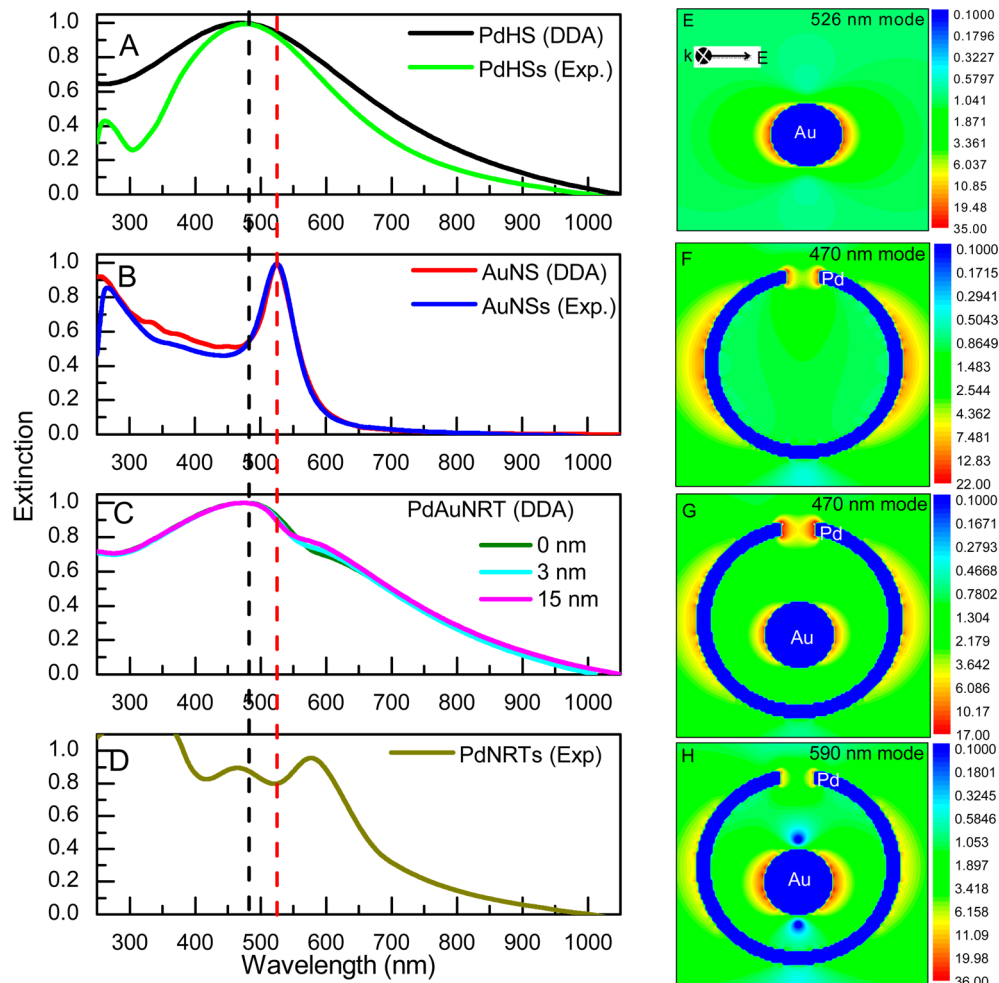


Figure 2. LSPR extinction spectrum of (A) 55.5 ± 6.3 nm palladium hollow nanospheres experimentally measured (green spectrum) and 77.5 nm palladium hollow nanospheres with 5 nm wall thickness calculated by DDA technique (black spectrum). (B) 29.8 nm gold nanospheres experimentally measured (blue spectrum) and calculated theoretically (red spectrum). (C) Palladium–gold nanorattles consist of 77.5 nm palladium nanoshell and 29.8 nm gold nanosphere when the inside separation distance between them is 0 (green spectrum), 3 (cyan spectrum), and 15 nm (magenta spectrum) calculated theoretically. (D) Measured for palladium–gold nanorattles of 29.8 ± 2.4 nm inside gold nanospheres and 77.5 ± 7.2 nm palladium outer nanoshells. It is clear that experimental results are in agreement with the theoretical results. The LSPR spectrum of the palladium nanoshells is broad, but the LSPR spectrum of the nanorattles is much broader and contains a dip suggesting the hybridization of plasmon resonance of the outer palladium nanoshell and gold nanosphere. The hybridization of the plasmon modes of the gold and palladium were also confirmed from the plasmon field contour calculations of: gold nanosphere (E) and palladium nanoshell excited at their resonance frequency (F), and palladium–gold nanorattles excited at 470 (G) and at 590 nm (H). The plasmon field on the gold nanosphere in the palladium–gold nanorattles when excited at 590 nm showed higher field intensity than that of the individual gold nanosphere when separated and excited at 526 nm, confirming the idea of the plasmon hybridization.

experimentally, which are verified theoretically by DDA technique when they are separated and in rattle structure. Figure 2A shows the LSPR spectrum measured for PdHNSs of 55.5 ± 6.3 nm in diameter and calculated for a single PdHNS of 77 nm diameter by DDA technique. It is clear from the theoretical and experimental results that PdHNSs show a single broad LSPR spectrum centered at ~ 470 nm. A single sharp single LSPR peak is obtained at 526 nm from the experimental measurement and the theoretically calculation for the 29.8 nm AuNSs (Figure 2B). Optical measurement of colloidal PdAuNRTs of 77.5 ± 7.2 nm outer PdHNSs with a 5 nm wall thickness and 29.8 ± 2.4 nm inner AuNSs showed broad plasmon with two peak maxima at 468 and 586 nm and a dip at 530 nm. (See Figure 2D.) It has been shown in a previous study that the inner AuNSs in the gold nanorattles move freely inside the gold hollow shells.²⁹ To study the effect of the separation distance between the inner AuNSs and the PdHNSs in the

PdAuNRTs, we carried out DDA calculation for the 77.5 nm PdAuNRTs of 5 nm wall thickness and 29.8 nm inner AuNS with the separation distances of 0 , 3 , and 15 nm. (See Figure 2C.) The LSPR spectrum of the PdAuNRT simulated by DDA was found to be slightly broader than that simulated for the separated PdHNS. In fact, upon increasing the inner separation distance, the width of the LSPR spectrum of the PdAuNRT increases, and the dip position is blue-shifted to 574 , 561 , and 546 nm when the distance is 0 , 3 , and 15 nm, respectively. Agreement between the measured and the calculated LSPR spectrum of the PdAuNRT is observed especially when a 15 nm inner separation distance between the PdHNS and AuNS is used in the calculation. On the basis of the above results, introducing AuNSs inside the PdHNSs increases the broadness of their LSPR spectrum and creates a dip in the LSPR spectrum close to the plasmon of AuNSs. The new feature of the LSPR spectrum of PdAuNRTs suggests the idea of hybridization of

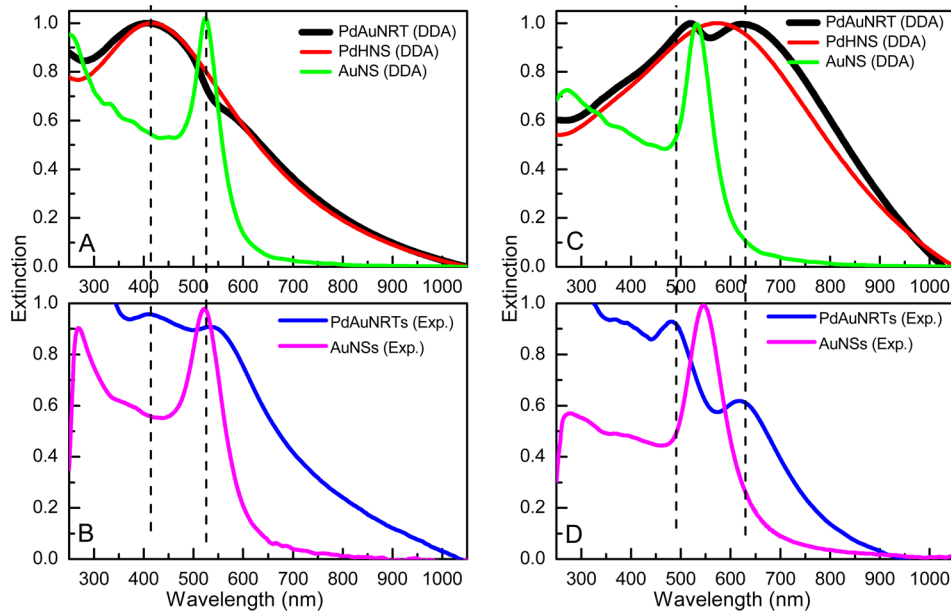


Figure 3. LSPR extinction spectrum. (A) Calculated by DDA technique for palladium–gold nanorattle (black) consists of palladium nanoshell of 41.6 nm diameter and 3 nm wall thickness (red spectrum is for palladium nanoshell when separated) and gold nanosphere of diameter of 16.5 nm (green spectrum is for the individual nanosphere). (B) Measured LSPR spectrum for 41.6 ± 5.2 nm palladium–gold nanorattles (blue spectrum) of 16.5 ± 2.5 nm inside gold nanospheres (magenta spectrum is measured for pure gold nanosphere). (C) Calculated for 148 nm palladium–gold nanorattle of 10 nm wall thickness (black), 65 nm gold nanosphere (green), and individual palladium nanoshell of (red). (D) Measured for palladium–gold nanorattles of diameter of 148 ± 15 nm (blue) and 65.1 ± 11.7 nm inner gold nanospheres (magenta spectrum is for pure gold nanospheres). It is clear that the LSPR spectrum of the nanorattles is much broader than that of the corresponding nanoshells due to hybridization of the plasmon resonance of gold nanospheres and palladium nanoshells, and the dip is found to be deeper for the larger sized nanorattles.

the plasmon resonance of AuNSs and PdHNSs. The hybridization of the plasmon modes of the AuNS and PdHNS in the PdAuNRT was confirmed by calculating the plasmon field contour for the AuNS and PdHNS when they are separated and in a rattle structure. The plasmon field was calculated at the resonance frequencies of individual AuNS and PdHNS and at wavelengths longer and shorter than that of the dip in case of PdAuNRT. Figure 2E shows the plasmon field distribution contour of AuNS excited at 526 nm. The field is distributed symmetrically on the surface of the nanosphere with high intensity in the same direction of polarization of the incident exciting field. PdHNS is characterized by the presence of inner and outer plasmonic surfaces. Figure 2F shows the plasmon field distribution contour of PdHNS when excited at 470 nm. The intensity of the plasmon field is high on the outer surface of the PdHNS and on the pores present on its wall, whereas no field was observed on the inner surface. When the PdAuNRT of 15 nm inner separation distance was excited at 470 nm, both the outer Pd nanoshell and the inner AuNS got excited and the field intensity increased on both the surface of AuNS and the outer surface of PdHNS. (See Figure 2G.) Interestingly, when the PdAuNRT is excited at 590 nm (photons with energy lower than that required for the excitation of individual AuNS), the plasmon field intensity on the surface of AuNS was found to be stronger than that on the surface of separated AuNS when excited at its the resonance frequency. However, the field intensity on the outer surface of the PdAuNRT was weaker than that of separated PdHNS. (See Figure 2H.) This unusual plasmon field distribution in the PdAuNRT would not be possible unless the plasmons of the AuNS and PdHNS undergo hybridization.

The plasmon resonance hybridization in the PdAuNRTs system was generalized by extending the discussion to cover

rattles with different sizes. Figure 3A shows the calculated LSPR extinction spectrum of 16.5 nm AuNS, 41.6 nm PdHNS of 3 nm wall thickness, and PdAuNRT of 7 nm separation distance between AuNS and PdHNS. The measured LSPR extinction spectrum of 16.5 ± 2.5 nm AuNSs and 41.6 ± 5.2 nm PdAuNRTs is shown in Figure 3B. The experimental results accorded well with the theoretical calculation. As previously observed, the LSPR spectrum of the PdAuNRT was broader than that of PdHNS, and dip appears close to the resonance frequency of AuNS. The same measurements and calculations were carried out for bigger nanorattles of 65 nm AuNS and 148 nm PdHNS with 10 nm wall length. The hybridization between the plasmon modes of PdHNSs and AuNSs is much clearer in this larger sized nanorattle. Furthermore, the dip in the extinction LSPR spectrum of PdAuNRTs is deeper, and the amount of broadness caused by the AuNS became more apparent. For more clarification of the plasmon resonance hybridization in the PdAuNRTs, it is worthy to apply the plasmon hybridization model to it.

PdAuNRTs are a complex plasmonic system, especially because the sharp LSPR spectrum of AuNSs overlaps with the broad LSPR of the palladium nanoshell when measured separately. The plasmon hybridization model is efficient to discuss such complex plasmonic systems.²¹ In the case of PdAuNRTs, the hybridization model is applied in two stages: the first is the plasmonic hybridization in the palladium nanoshell, which is not much different from what has been previously reported for gold nanoshell.²¹ The second stage is the hybridization of the plasmon modes of the inner gold sphere and that of palladium nanoshell.

The palladium nanoshell has inner and outer plasmonic surfaces, which can be considered as a combination of a palladium nanosphere and palladium nanocavity. When the

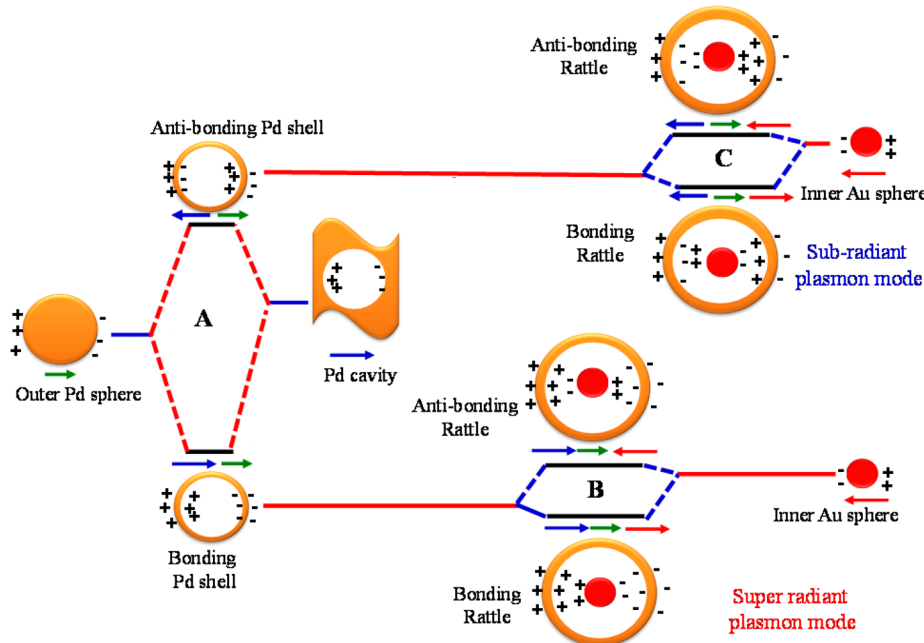


Figure 4. Schematic diagram that describes the hybridization of the plasmon resonance in (A) a palladium hollow nanosphere that is treated as a combination of a solid palladium nanosphere and palladium nanocavity; the bonding plasmon mode is obtained with low energy and a large value of the dipole moment, and antibonding mode for the interaction leads to high energy. The large value of dipole moment explains the observed broad LSPR spectrum of palladium hollow nanosphere. (B) Palladium–gold nanorattle, however the bonding plasmon mode is obtained with low energy and the highest value of the dipole moment (super radiant) when the bonding mode of a palladium hollow nanosphere is mixed with the plasmon mode of the inner AuNS. (C) For palladium–gold nanorattle, the bonding dark plasmon mode (subradiant) is obtained when the antibonding plasmon mode of palladium hollow nanosphere is mixed with the plasmon mode. The large value of dipole moment in the palladium–gold nanorattle compared with that in the palladium hollow nanosphere explains the increase in width of the LSPR spectrum of the nanorattles compared with the LSPR of the palladium hollow nanospheres. The dip in the LSPR spectrum of palladium–gold nanorattles is due to the interference of narrow subradiant dark plasmon mode with the broad super-radiant plasmon modes of the nanorattles.

palladium nanosphere and the nanocavity are excited with an incident field polarized along their axis, an electron cloud and dipoles are generated in the same direction of polarization on both the surface of nanosphere and in the nanocavity as well. Upon hybridization of the plasmon modes of the nanosphere and nanocavity in PdHNS, a low-energy bonding plasmon mode is formed when the electron cloud on the surface of the nanosphere and the nanocavity are arranged to be electrostatically attractive. This leads to the in-phase alignment of the dipoles (head-to-tail), resulting in a large value of the net dipole moment. A high-energy antibonding plasmon mode is suggested for the alignment of the electron clouds undergoing repulsion, which causes out-of-phase alignment of the dipoles (head-to-head) and a lower value of the dipole moment. (See Figure 4A.)

When AuNS is introduced inside the PdHNS in the PdAuNRT, the excitation of the AuNS electron cloud will generate a dipolar charge on its surface. The plasmon mode of AuNS hybridizes with both the bonding and antibonding modes of the PdHNS. Although the antibonding mode of the PdHNS is forbidden, when AuNS is introduced inside the PdHNS the net electrostatic charges on the inner and the outer surfaces of the PdHNS will be changed.

When the plasmon mode of AuNS is hybridized with the bonding plasmon mode of the PdHNS, a low-energy bonding plasmon mode will be obtained upon alignment of all negative charges on the inner and outer surfaces of the PdHNS and on the outer surface of the AuNS, in the same direction. In fact, such alignment resulted in an in-phase alignment of the dipoles producing maximum value of the net dipole moment (bottom

part in Figure 4B). In addition to the low-energy bonding mode, a higher energy antibonding mode is assumed when the charge on the surface of AuNS is switched to the opposite direction. This alignment offers out-of-phase dipoles with a low value of dipole moment (top part in Figure 4B).

When the plasmon modes of a AuNS and the antibonding plasmon mode of a PdHNS undergo hybridization, upon alignment of the AuNS surface charge to be opposite to that on the inner surface of the PdHNS, the net repulsive force on the antibonding mode of PdHNS will be decreased, and a bonding plasmon mode for PdAuNRT is obtained with lower energy. The value of the net dipole moment in this case is small (bottom part in Figure 4C). Finally, when the charge on the surface of AuNS is switched to be similar to that on the inner surface of PdHNS, the high energy forbidden antibonding mode is proposed (top part Figure 4C).

The width of the LSPR extinction spectrum of any plasmonic nanoparticle is proportional to the damping rate of the dipolar charge oscillation,⁵ which is proportional to the square of the second derivative of the dipole moment.⁵ Applying this to the PdHNS, the bonding mode has a large value of the net dipole moment, which causes the broadening of its LSPR spectrum. In the case of a PdAuNRT system, the bonding plasmon mode of lower energy presented a huge value of the dipole moment, larger than that for the individual PdHNS, which explains the reason for the increased the width of the LSPR spectrum of PdAuNRTs compared with the PdHNSs. The reason for the observed dip in the LSPR spectrum of the PdAuNRTs can be described as follow: based on the hybridization model, PdAuNRTs have two bonding plasmon modes, one with low

energy and a large value of dipole moment (a bright, super-radiant, broad plasmon mode) and the other has high energy and a low value of dipole moment, considered as a subradiant dark plasmon mode (narrow width). The interference between the bright broad mode and the narrow dark plasmon mode resulted in the formation of the dip in the LSPR spectrum of PdAuNRT and a Fano resonance.

Palladium and gold metals are combined on the nanoscale forming an exciting bimetallic nanorattle. This approach, based on the galvanic replacement technique, was used to prepare palladium–gold nanorattles with different sizes. Spherical gold–silver core–shell nanoparticles were prepared first. Two silver atoms in the shell around the gold nanosphere were replaced by one palladium atom, resulting in the generation of vacant nanoshell surrounding the small gold nanosphere. Both gold nanospheres and palladium nanoshells are characterized by the presence of single localized surface plasmon resonance spectra, which is sharp for gold nanospheres and broad for palladium nanoshells when measured separately. Interestingly, the plasmon modes of palladium nanoshells and gold nanospheres hybridized when they are combined in the palladium–gold nanorattles. This hybridization leads to broadening of the LSPR spectrum of the palladium–gold nanorattles and the formation of a dip in the center of the spectrum, observed experimentally and confirmed by the DDA technique for nanorattles of different sizes. The broadening of the LSPR spectrum of the palladium–gold nanorattles is due to the formation of a super-radiant bright plasmon mode, with an enhanced value of the net dipole moment. A subradiant, narrow plasmon mode is also suggested in the rattles with a low dipole moment. Interference between the bright and dark plasmon mode resulted in the formation of the dip in the LSPR spectrum.

ASSOCIATED CONTENT

Supporting Information

Detailed experimental procedures used for the synthesis of palladium hollow nanospheres and palladium gold nanorattles of different sizes. This material is available free of charge via the Internet at <http://pubs.acs.org>.

AUTHOR INFORMATION

Corresponding Author

*E-mail: mmahmoud@gatech.edu.

Notes

The authors declare no competing financial interest.

ACKNOWLEDGMENTS

This work was supported by the NSF grant (1306269). I would like to thank Mr. B. Garlyev and Mr. J. Broadly for helping in TEM imaging.

REFERENCES

- (1) Maier, S. A. *Plasmonics: Fundamentals and Applications*; Springer: New York, 2007.
- (2) Jeanmaire, D. L.; Vanduyne, R. P. Surface Raman Spectroelectrochemistry 0.1. Heterocyclic, Aromatic, and Aliphatic-Amines Adsorbed on Anodized Silver Electrode. *J. Electroanal. Chem.* **1977**, *84*, 1–20.
- (3) Halas, N. J.; Lal, S.; Chang, W. S.; Link, S.; Nordlander, P. Plasmons in Strongly Coupled Metallic Nanostructures. *Chem. Rev.* **2011**, *111*, 3913–3961.

(4) Mahmoud, M. A.; El-Sayed, M. A. Aggregation of Gold Nanoframes Reduces, Rather than Enhances, SERS Efficiency due to the Trade-off of the Inter-and Intraparticle Plasmonic Fields. *Nano Lett.* **2009**, *9*, 3025–3031.

(5) Kelly, K. L.; Coronado, E.; Zhao, L. L.; Schatz, G. C. The Optical Properties of Metal Nanoparticles: The Influence of Size, Shape, and Dielectric Environment. *J. Phys. Chem. B* **2003**, *107*, 668.

(6) Mahmoud, M. A.; Poncheri, A. J.; Phillips, R. L.; El-Sayed, M. A. Plasmonic Field Enhancement of the Exciton–Exciton Annihilation Process in a Poly (p-phenyleneethynylene) Fluorescent Polymer by Ag Nanocubes. *J. Am. Chem. Soc.* **2010**, *132*, 2633–2641.

(7) Wadams, R. C.; Yen, C. W.; Butcher, D. P., Jr.; Koerner, H.; Durstock, M. F.; Fabris, L.; Tabor, C. E. Gold Nanorod Enhanced Organic Photovoltaics: The Importance of Morphology Effects. *Org. Electron.* **2014**, *15*, 1448–1457.

(8) Huang, X.; El-Sayed, I. H.; Qian, W.; El-Sayed, M. A. Cancer Cell Imaging and Photothermal Therapy in the Near-Infrared Region by Using Gold Nanorods. *J. Am. Chem. Soc.* **2006**, *128*, 2115–2120.

(9) Burda, C.; Chen, X. B.; Narayanan, R.; El-Sayed, M. A. Chemistry and Properties of Nanocrystals of Different Shapes. *Chem. Rev.* **2005**, *105*, 1025–1102.

(10) Jana, N. R.; Gearheart, L.; Murphy, C. J. Wet Chemical Synthesis of High Aspect Ratio Cylindrical Gold Nanorods. *J. Phys. Chem. B* **2001**, *105*, 4065–4067.

(11) Sisco, P. N.; Murphy, C. J. Surface-Coverage Dependence of Surface-Enhanced Raman Scattering from Gold Nanocubes on Self-Assembled Monolayers of Analyte. *J. Phys. Chem. A* **2009**, *113*, 3973–3978.

(12) Mahmoud, M. A.; O’Neil, D.; El-Sayed, M. A. Hollow and Solid Metallic Nanoparticles in Sensing and in Nanocatalysis. *Chem. Mater.* **2014**, *26*, 44–58.

(13) Lohse, S. E.; Burrows, N. D.; Scarabelli, L.; Liz-Marzán, L. M.; Murphy, C. J. Anisotropic Noble Metal Nanocrystal Growth: The Role of Halides. *Chem. Mater.* **2013**, *26*, 34–43.

(14) Gupta, M. K.; König, T.; Near, R.; Nepal, D.; Drummey, L. F.; Biswas, S.; Naik, S.; Vaia, R. A.; El-Sayed, M. A.; Tsukruk, V. V. Surface Assembly and Plasmonic Properties in Strongly Coupled Segmented Gold Nanorods. *Small* **2013**, *9*, 2979–2990.

(15) Koenderink, A. F.; Polman, A. Complex Response and Polariton-Like Dispersion Splitting in Periodic Metal Nanoparticle Chains. *Phys. Rev. B* **2006**, *74*, 033402–033406.

(16) Hodak, J. H.; Martini, I.; Hartland, G. V. Spectroscopy and Dynamics of Nanometer-Sized Noble Metal Particles. *J. Phys. Chem. B* **1998**, *102*, 6958–6967.

(17) Niu, Z.; Zhen, Y.-R.; Gong, M.; Peng, Q.; Nordlander, P.; Li, Y. Pd Nanocrystals with Single-, Double-, and Triple-Cavities: Facile Synthesis and Tunable Plasmonic Properties. *Chem. Sci.* **2011**, *2*, 2392–2395.

(18) Mahmoud, M. A. Surface-Enhanced Raman Spectroscopy of Double-Shell Hollow Nanoparticles: Electromagnetic and Chemical Enhancements. *Langmuir* **2013**, *29*, 6253–6261.

(19) Popa, A.; Samia, A. C. S. Effect of Metal Precursor on the Growth and Electrochemical Sensing Properties of Pt-Ag Nanoboxes. *Chem. Commun.* **2014**, *50*, 7295–7298.

(20) Mahmoud, M. A.; Szymanski, P.; El-Sayed, M. A. Different Methods of Increasing the Mechanical Strength of Gold Nanocages. *J. Phys. Chem. Lett.* **2012**, *3*, 3527–3531.

(21) Prodan, E.; Radloff, C.; Halas, N. J.; Nordlander, P. A Hybridization Model for the Plasmon Response of Complex Nanostructures. *Science* **2003**, *302*, 419–422.

(22) Lassiter, J. B.; Sobhani, H.; Fan, J. A.; Kundu, J.; Capasso, F.; Nordlander, P.; Halas, N. J. Fano Resonances in Plasmonic Nanoclusters: Geometrical and Chemical Tunability. *Nano Lett.* **2010**, *10*, 3184–3189.

(23) Fan, J. A.; Wu, C. H.; Bao, K.; Bao, J. M.; Bardhan, R.; Halas, N. J.; Manoharan, V. N.; Nordlander, P.; Shvets, G.; Capasso, F. Self-Assembled Plasmonic Nanoparticle Clusters. *Science* **2010**, *328*, 1135–1138.

- (24) Zou, W.-B.; Z, J.; Li, Jin; Zhang, H.-P. Properties of Localized Surface Plasmon Resonance of Gold Nanoshell Pairs. *Acta Phys. Sin.* **2012**, *61*, 97805–097805.
- (25) Sonnefraud, Y.; Verellen, N.; Sobhani, H.; Vandenbosch, G. A. E.; Moshchalkov, V. V.; Van Dorpe, P.; Nordlander, P.; Maier, S. A. Experimental Realization of Subradiant, Superradiant, and Fano Resonances in Ring/Disk Plasmonic Nanocavities. *ACS Nano* **2010**, *4*, 1664–1670.
- (26) Lovera, A.; Gallinet, B.; Nordlander, P.; Martin, O. J. F. Mechanisms of Fano Resonances in Coupled Plasmonic Systems. *ACS Nano* **2013**, *7*, 4527–4536.
- (27) Brown, L. V.; Sobhani, H.; Lassiter, J. B.; Nordlander, P.; Halas, N. J. Heterodimers: Plasmonic Properties of Mismatched Nanoparticle Pairs. *ACS Nano* **2010**, *4*, 819–832.
- (28) Bigelow, N. W.; Vaschillo, A.; Camden, J. P.; Masiello, D. J. Signatures of Fano Interferences in the Electron Energy Loss Spectroscopy and Cathodoluminescence of Symmetry-Broken Nanorod Dimers. *ACS Nano* **2013**, *7*, 4511–4519.
- (29) Mahmoud, M. A. Optical Properties of Gold Nanorattles: Evidences for Free Movement of the Inside Solid Nanosphere. *J. Phys. Chem. C* **2014**, *118*, 10321–10328.
- (30) Freund, P. L.; Spiro, M. Colloidal Catalysis - the Effect of Sol Size and Concentration. *J. Phys. Chem.* **1985**, *89*, 1074–1077.